International Journal of Microwave and Wireless Technologies, 2009, 1(2), 153–160.
doi:10.1017/S1759078709990444 Printed in the United Kingdom

Self-heating phenomena in high-power III-N transistors and new thermal characterization methods developed within EU project TARGET

JAN KUZMIK[1,7], SERGEY BYCHIKHIN[1], EMMANUELLE PICHONAT[2], CHRISTOPHE GAQUIÈRE[3], ERWAN MORVAN[4], ERHARD KOHN[5], JEAN-PIERRE TEYSSIER[6] AND DIONYZ POGANY[1]

In the framework of the Top Amplifier Research Groups in a European Team (TARGET) project, we developed a new electrical method for the temperature measurement of HEMTs and performed several unique studies on the self-heating effects in AlGaN/GaN HEMTs. This method, in combination with transient interferometric mapping (TIM), provides a fundamental understanding of the heat propagation in a transient state of HEMTs. The AlGaN/GaN/Si HEMT thermal resistance was determined to be ~70 K/W after 400 ns from the start of a pulse, and the heating time constant was ~200 ns. Our experimental methods were further applied on multifinger high-power AlGaN/GaN/sapphire HEMTs. The TIM method indicates that the airbridge structure serves as a cooler, removing approximately 10% of the heat energy. In the next study we used TIM and the micro-Raman technique to quantify thermal boundary resistance (TBR) between different wafer materials and GaN epi-structure. We found TBR to be ~7 × 10^{-8} m^2K/W for GaN/Si and ~1.2 × 10^{-7} m^2K/W for GaN/SiC interfaces. The role of TBR at the GaN/sapphire interface was found to be less important.

Keywords: Self-heating, Temperature measurements, High-electron-mobility transistors, AlGaN/GaN

Received 29 May 2009; Revised 5 June 2009

I. INTRODUCTION

III-N semiconductors are becoming a top material choice for future telecommunication amplifiers. Applications in which high power and frequency performance are to be achieved together with a high linearity and reliability of systems require efficient transistor cooling. Indeed, understanding and measuring a self-heating effect is becoming increasingly important as devices are becoming smaller and power densities higher.

AlGaN/GaN HEMT operation up to 600°C without irreversible damage has been documented [1, 2]. However, it was shown that elevated temperature instantaneously decreases channel electron mobility [1–4], decreases maximal drain current [2], increases gate leakage [2], and degrades transistor RF performance [1]. The role of AlGaN/GaN HEMT effective cooling from the side of the substrate (on which the device is grown) has been described in [5]. Particular attention has recently been devoted to the investigation of thermal coupling at the III-nitride/substrate interface [6–9]. A difference in the acoustic impedance of materials forming the interface gives the level of thermal coupling and determines thermal boundary resistance (TBR) [8, 9]. However, it was also pointed out that dislocations at the interface, such as dangling bonds at the AlN/Si junction [10], might give rise to an additional increase in TBR [6]. Substantial device "overheating" [7] and performance degradation due to TBR was reported [8]. The value of TBR was measured to be 7–8 × 10^{-8} m^2K/W for the AlN/Si interface at room temperature [6] and 1 × 10^{-4} m^2K/W for GaN/sapphire at 4.2 K [9] (representing 1–5 × 10^{-7} m^2K/W at 300 K [8]).

Alternatively, the HEMT temperature can be reduced by heat removal from the top. It was shown that heat removal either through the epoxy fill [11] or through properly designed bumps [12] of the flip-chip mounted multifinger AlGaN/GaN/sapphire HEMTs can effectively decrease the device thermal impedance without using expensive SiC substrate.

Steady-state temperature in the AlGaN/GaN HEMT has previously been investigated using optical methods such as micro-Raman [13], micro-photoluminescence [14], IR microscopy [15], and liquid crystal thermography [16] or using the electrical direct current (DC) characterization method [17]. Numerical models were used in the same reports to validate experiments, assuming k to be dependent on [13, 18, 16] or independent (linear model) [14] of

[1]Institute for Solid-State Electronics, TU Vienna, Floragasse 7, A-1040 Vienna, Austria. Phone: +43 1 58801 36215; Fax: +43 1 58801 362 99.
[2]LASIR UMR 8516 USTL, 59655 Villeneuve d'Ascq cedex, France.
[3]IEMN, av. Poincaré, BP 69, 59652 Villeneuve d'Ascq, France.
[4]Alcatel-Thales III-V Lab/TIGER, 91404 Orsay, France.
[5]Department of Electron Devices and Circuits, University of Ulm, 89081 Ulm, Germany.
[6]IRCOM CNRS University of Limoges, 7 rue Jules Valles, 19100 Brive, France.
[7]Institute of Electrical Engineering, Slovak Academy of Science, Dubravska cesta 9, 842 39 Bratislava, Slovakia.
Corresponding author:
J. Kuzmik
Email: jan.kuzmik@tuwien.ac.at

temperature. More recently, a transient interferometric mapping (TIM) technique [19] has been demonstrated as a valuable tool for tracing the dissipated energy in AlGaN/GaN HEMTs [15] in the transient state. The TIM technique has also been applied for extracting power density distributions, mapping current filaments in silicon devices under electrostatic discharge stress [20].

Within the Top Amplifier Research Groups in a European Team (TARGET) project we developed an electrical method for the determination of temperature in a transient self-heating state of HEMTs (i.e. as in a pulsed regime) [21]. We present the results of AlGaN/GaN HEMTs grown on silicon. Experiments are correlated with the results of the two-dimensional (2D) thermal model and the value of TBR at the interface with silicon substrate is estimated by model fitting. Optical experiments and thermo-optical modeling further independently validate the determined transistor temperature and TBR values.

In the next study we investigated the transient temperature rise in multifinger AlGaN/GaN/sapphire HEMTs subjected to 10 μs voltage pulses [22]. In particular we investigated the role of the airbridge structure in device thermal management. Airbridge technology is used in high-power HEMTs to connect parallel source contacts in a multifinger layout. Finally we studied TBR and its effect on thermal management in the transfer length method (TLM) GaN HEMT test structures grown alternatively on three kinds of commonly used substrate materials: Si, SiC, and sapphire [23]. The temperature drop at the III-nitride/Si interface is investigated by using a micro-Raman spectroscopy technique under DC conditions. TBR at the III-nitride/SiC and III-nitride/sapphire interfaces is characterized in transient mode by TIM.

II. METHODS AND STRUCTURES

A) Electrical characterization method

The transient electrical method of temperature determination in the process of self-heating was developed from the DC steady-state characterization method [17]. The DC steady-state method was based on the effect of the HEMT drain current drop $\Delta I_{sat}(V_D)$ as the drain voltage is increased. This effect was described analytically by [17]

$$\Delta I_{sat}(V_D) = -g_m(I_{sat}\Delta R_S + \Delta V_T) + I_{sat}\Delta v_{sat}/v_{sat} + V_D/R_{sub}, \quad (1)$$

where g_m is transconductance, and ΔR_S, ΔV_T, and Δv_{sat} are temperature-driven changes in the source resistance, threshold voltage, and electron saturation velocity, respectively. V_D represents drain voltage and R_{sub} represents leakage through the buffer layer. Calibrating the steady-state dependencies of transistor parameters on temperature (ΔR_S and $\Delta V_T = f(T)$, Δv_{sat} was neglected), it is possible to determine the HEMT channel temperature as a function of dissipated power $V_D \times I_{sat}$.

To investigate self-heating in the transient state, we applied a transmission line pulser (TLP) to bias the HEMT drain contact (the source and the gate were grounded during the pulse). In the TLP technique a coaxial cable (TL) with a 50 Ω characteristic impedance was charged by a voltage source and later discharged by closing a relay, providing rectangular voltage pulses. Different values of the charging voltage were used while a pulse duration of 480 ns was fixed as given by the cable length. The current and voltage waveforms on the drain were recorded using a digital oscilloscope.

To describe a temperature-induced *time-dependent* current drop $\Delta I_{sat}(t)$, we used methodology of the DC method, taking into account several differences. First of all, as the voltage is kept constant during the pulse, the same is assumed for the buffer leakage current and the last term in (1) can be omitted. Secondly, it is necessary to take into account that the calibration of HEMT parameters ($\Delta R_S = f(T)$, $\Delta V_T = f(T)$) is always performed in the steady state, while the method is transient. The change of HEMT source resistance $\Delta R_S = f(T)$ may be related to the decreased electron mobility with temperature. Similarly to the DC case we neglect Δv_{sat}, introducing approx. 10% error in the temperature determination [17]. Consequently, $\Delta I_{sat}(t)$ can be expressed as

$$\Delta I_{sat}(t) = -g_m I_{sat}\Delta R_S. \quad (2)$$

To obtain $\Delta R_S = f(T)$ dependence, the device was gradually heated using an external heater up to 250°C. R_S was measured at low drain current so that the low dissipated power (~50 mW/mm) minimized the self-heating. Using a polynomial fit of the calibration curves $R_S = f(T)$ and $g_m(T) = g_m(300\text{ K})/[1 + g_m(300\text{ K}) \times \Delta R_S(T)]$ together with the measured $\Delta I_{sat}(t)$, an iterative solution of (2) was performed to obtain channel temperature transient characteristics.

B) Micro-Raman measurements

Micro-Raman measurements were performed using a Labram micro-Raman system [24]. The temperature dependence of semiconductor phonon frequencies and Stokes/anti-Stokes peak intensity [25] was used for calibration, in which an externally heated sample was probed by a laser beam of the Raman system. The temperature increase due to the self-heating effect in the AlGaN/GaN/Si HEMT test structure was investigated afterwards by comparing the phonon frequencies. For the 514.5 nm line of an argon ion laser beam, the GaN layer is transparent. However, for the given wavelength the beam is strongly absorbed in the Si substrate (which is not the case for SiC and sapphire substrates) with an absorption coefficient of $0.76 \times 10^4\ \text{cm}^{-1}$ [26]. Consequently, by applying the probe beam from the device topside, we can investigate temperature discontinuity ΔT at the III-nitride/Si interface by obtaining the information both from GaN and from a part of the Si substrate 1–2 μm from the interface.

C) Transient interferometric scanning method

The scanning TIM method was based on measuring temperature-induced changes in a semiconductor refractive index from the device backside, using a probe laser beam ($\lambda = 1.3$ μm). The beam reflected from the device topside undergoes an optical phase shift $\Delta\varphi(t)$, which is measured interferometrically by combining the probe beam (located in the heated area) with an unperturbed reference beam (another branch of the interferometer); see Fig. 1. The phase shift is a sum of two contributions, $\Delta\varphi_{GaN}$ and $\Delta\varphi_{sub}$, that

https://doi.org/10.1017/S1759078709990444 Published online by Cambridge University Press

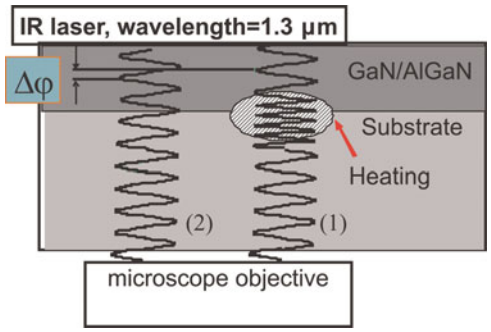

Fig. 1. Laser interferometer measuring principle. The substrate and III-nitrides epistructure refractive indexes are changes due to the device self-heating. A probe beam (1) and a reference beam (2) are combined in an interferometer. The phase of the probe beam changes due to the self-heating effect (exaggerated for visibility).

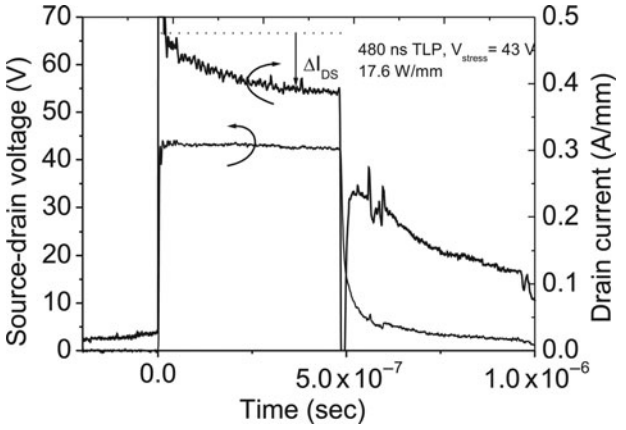

Fig. 2. HEMT current–voltage waveforms during 43 V pulse applied on the drain. After [21].

are proportional to the integral of temperature distribution $T(x,y,z)$ along the beam path (z-axis) in GaN or substrate, respectively, weighted by dn/dT:

$$\Delta\varphi(x, y, t) = \Delta\varphi_{\mathrm{GaN}}(x, y, t) + \Delta\varphi_{sub}(x, y, t) = \frac{4\pi}{\lambda}\frac{dn}{dT}\bigg|_{\mathrm{GaN}}\int_{\mathrm{GaN}}\Delta T(x, y, z, t)dz + \frac{4\pi}{\lambda}\frac{dn}{dT}\bigg|_{sub}\int_{sub}\Delta T(x, y, z, t)dz. \quad (3)$$

The TIM method operates in the transient (pulsed) regime of the self-heated device with a ns time and 1.5 μm space resolution.

D) Simulation

The Matlab toolbox was used for 2-D numerical thermo-optical simulation. Because of numerical reasons and meshing, TBR at the III-nitride/substrate interface in the model was represented by a virtual 100 nm thick thermal insulation layer with thermal conductivity k_{ISO} (i.e. TBR = 100 nm/k_{ISO}). Adiabatic boundary conditions were assumed for calculations in the transient state. However, for a steady-state simulation we considered 300 μm thick substrate with isothermal (300 K) condition at the backside.

Quantitative evaluation of TBR is based on the comparison of measured $\Delta\varphi(t)$ dependencies with the corresponding quantities calculated using the thermal simulation and equation (3). TBR and dn/dT are taken as fitting parameters. In the thermal model, the source–drain distance defines the device heat dissipation area. 100 nm thick GaN insulation layers (ISO) represent regions where lattice dislocations and/or TBR are decisive. Thermal conductivities of ISOs, $k_{ISO1,2}$, were used as fitting parameters of the thermal model.

III. RESULTS

A) Transient self-heating in AlGaN/GaN/Si HEMTs

In Fig. 2 we show current and voltage waveforms of devices under 43 V TLP pulse. The HEMT channel temperature increase was determined using the described electrical characterization method and equation (2). Results shown in Fig. 3 are compared with calculated transients. Fitting of the experiment indicates TBR $\sim 7 \times 10^{-8}$ m^{2}K/W. The calculated temperature increase is by about 10% higher than the measured one at the end of the pulse. Several reasons may account for this: the fact that Δv_{sat} is neglected (~10% error), simplifications introduced by the model/experiment, and less established physical parameters of III-nitride materials. Nevertheless, the comparison of the experiment with the model with and without ISOs clearly indicates the presence of the thermally insulating layers.

Calculating the average dissipated power over the 400 ns time interval for different voltage levels, we could construct the experimental dependence of HEMT channel temperature (after 400 ns) on delivered power, shown in Fig. 4. Depicted points indicate almost linear dependence $\Delta T = f(P/w)$ and, thus, for a selected time instant a device thermal resistance $R_{th} = \Delta T(t)/P$ was independent of dissipated power. We obtained $R_{th} = \sim 70$ K/W at $t = 400$ ns. From the temperature exponential behavior in Fig. 3, one can also estimate the heating time constant (approx. 190 ns).

The role of insulation layers is further illustrated in Figs 5(a) and 5(b), where temperature profiles are calculated

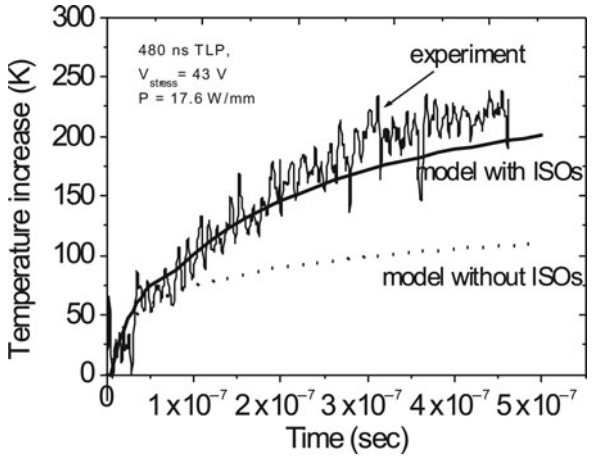

Fig. 3. Experimental and calculated (with and without ISOs) temperature increase after a 43 V pulse of 480 ns duration. After [21].

https://doi.org/10.1017/S1759078709990444 Published online by Cambridge University Press

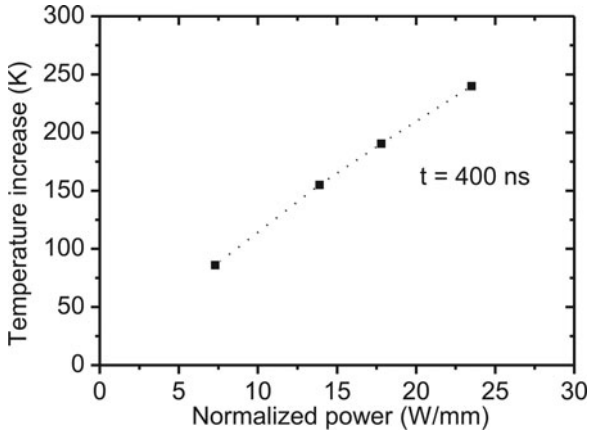

Fig. 4. Experimental temperature increase as a function of normalized dissipated power at $t = 400$ ns. After [21].

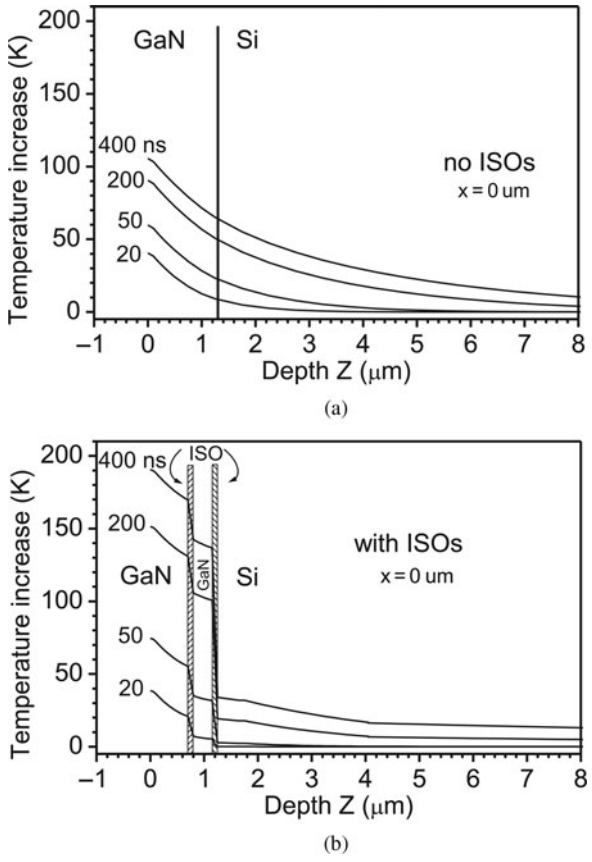

Fig. 5. Calculated temperature increase profiles in AlGaN/GaN/Si HEMT (a) without and (b) with ISO, at different time instances. After [21].

for HEMTs with and without ISOs being considered. A dominant effect of TBR is visible (Fig. 5(b)). After 400 ns the device with ISOs exhibited a surface temperature increase of more than 190 K, by ~80 K more as if ISOs are not present.

B) Self-heating in multifinger AlGaN/GaN HEMTs

To investigate heat dissipation in multifinger HEMTs (see Fig. 6), we used the TIM technique. Figure 7 shows the

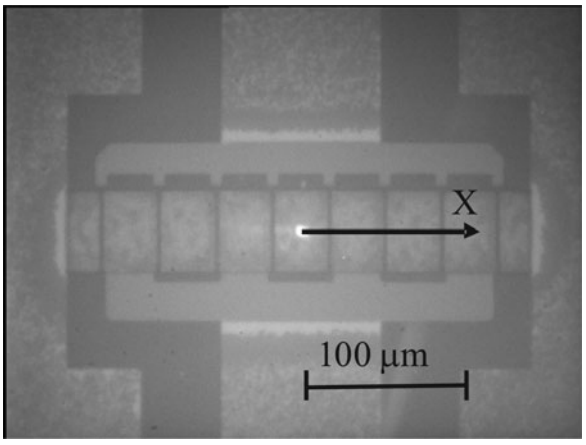

Fig. 6. Back side infrared camera image of the multifinger AlGaN/GaN HEMT. Laser beam is visible in the center, scanning was performed along the x-axis. After [22].

evolution of phase shift profiles taken during a 10 μs/10 V pulse at $t = 2$, 6, and 10 μs, and after the pulse at $t = 30$ μs. As expected, the $\Delta\varphi(x)$ signal increases during the pulse due to heating and decreases after the pulse due to cooling, thus reflecting the heat dynamics in the device. The spreading of peaks with time can also be observed due to lateral heat diffusion. The difference in the evolution of the signal magnitude in the valleys marked by arrows A, B (Fig. 7) is remarkable. At position 'A', a source contact with the electroplated thick gold metal on it is localized, while an ordinary drain contact is located at 'B'. At $t = 2$ μs one observes nearly the same small amplitude $\Delta\varphi_B \sim \Delta\varphi_A$; however, for $t > 2$ μs the phase shift at the ordinary drain contact is higher $\Delta\varphi_B > \Delta\varphi_A$. The difference vanishes after the pulse is terminated ($t = 30$ μs). To interpret this result, we take into account that the phase shift represents only the heat energy in the semiconductor and the substrate, but not that which is transferred from semiconductor to metallization. Then the deeper valleys at position 'A' originate from a better heat sinking at the location of airbridges compared to the ordinary drain

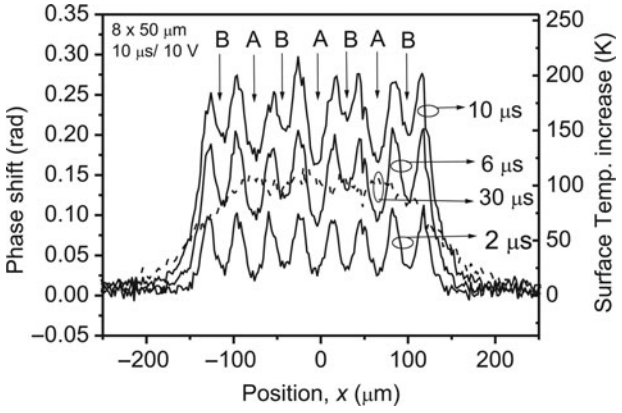

Fig. 7. Phase shift evolution (left side vertical scale) and extracted surface temperature increase (right side scale) profiles of the AlGaN/GaN HEMT stressed by 10 V/10 μs drain pulse. The temperature scale holds only for the data at $t = 2$ and 6 μs, the dashed line depicts phase shift signal after the pulse at $t = 30$ μs. Positions A mark the signal minimum at the source contacts with airbridge connections, positions B mark the signal at the ordinary drain contacts. After [22].

https://doi.org/10.1017/S1759078709990444 Published online by Cambridge University Press

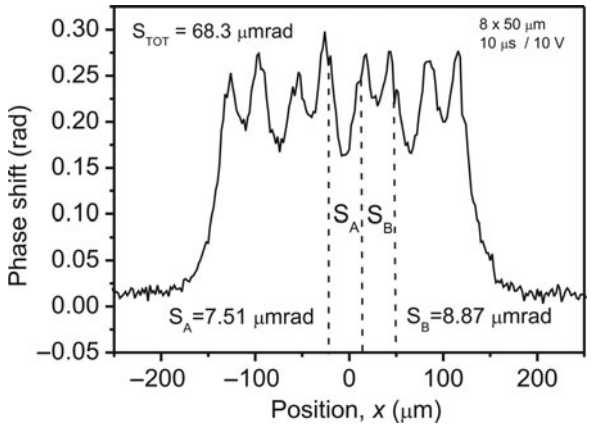

Fig. 8. Phase shift profiles of the HEMT of Fig. 3 at $t = 10$ μs with marked areas S_A and S_B below the source and the drain contacts. After [22].

contact. This effect is negligible for the short time instants ($t < 2$ μs), and becomes more visible at longer time when heat penetrates more effectively from the active region to the thick metal airbridge.

To estimate the amount of heat transferred via the airbridge at $t = 10$ μs, we calculate the difference of "areas" S_A and S_B below the $\Delta\varphi$ signal at contacts, which are proportional to the total dissipated heat; see Fig. 8. The difference of areas was approx. 1.35 μm rad. Taking into account the total area $S_{TOT} \sim 68$ μm·rad and that the number of airbridge contacts is five, the airbridge cooling efficiency η, i.e. the percentage of the total heat transferred from the device to the airbridge, can be estimated as $\eta = 5 \times (S_B - S_A)/S_{TOT} \sim 10\%$. A similar ratio of ~10% was obtained also at $t = 6$ μs, but ~3% at $t = 2$ μs. Thus it seems that after the initial increase, the cooling efficiency η of the airbridge contacts saturates. The saturation can be explained by the merging of heat waves ($\Delta\varphi$ signals) from neighboring channels at $t \sim 6$ μs.

We present the approach of how to determine temperature maps $\Delta T_{surface}(x)$ from the combination of TIM measurements and the knowledge of the $\Delta T_{channel}$ value extracted by the electrical method. We first relate the phase shift $\Delta\varphi$ (x) to the GaN surface temperature $\Delta T_{surface}$ at the particular time instant. The profiles for $t \sim 2$–6 μs are the most flat and the difference between the peak and the valley of the $\Delta T_{surface}(x)/\Delta\varphi(x)$ distribution is less than 15% (not shown). Consequently, if $\Delta T_{channel}$ is known in this time scale, the temperature profile maps can be obtained from TIM phase measurements. Taking into account our results of $\Delta T_{channel}$ determination (see Fig. 9) and TIM experiments (see Fig. 7, left $\Delta\varphi$ scale) and provided that $\Delta T_{channel}/\Delta\varphi_{channel} \sim$ 730 K/rad at both $t = 2$ and 6 μs, the phase shift scale of Fig. 7 can be directly transformed into the temperature scale (see right scale, consider only the data at $t = 2$ and 6 μs). At $t = 6$ μs one can observe an ~25 K difference between the temperature in the center of the source (position A) and the drain (position B) contacts, representing a 25% change.

C) Investigation of TBR at different III-nitride/substrate interfaces

Figure 10 shows a steady-state dependence of temperature T on dissipated power density P_{2D} $(= V \times I)$/area at the GaN/Si interface extracted by the micro-Raman measurements. One can observe a linear increase of $\Delta T = T_{GaN} - T_{Si}$ with P_{2D}, where T_{GaN} and T_{Si} are the temperatures at the GaN and Si sides of the interface. We estimate TBR as $\Delta T/P_{2D}$, giving a value of $\sim 7 \times 10^{-8}$ m²K/W. This value is in very good agreement with our previous study [$TBR_{GaNonSi} \sim 7$–8×10^{-8} m²K/W] using TIM [21].

Figures 11(a) and 11(b) show the experimental and modeled $\Delta\varphi$ transients of the studied GaN/SiC TLM device for different values of $(dn/dT)_{GaNonSiC}$ and $(TBR)_{GaN/SiC}$. Constant power $P_{2D} \sim 8.2$ mW/μm² is dissipated in TLM devices for 500 ns. The best fitting of the data is obtained for $(dn/dT)_{GaNonSiC} = 5.2 \times 10^{-5}$ K^{-1} and $(TBR)_{GaN/SiC} = 1.2 \times 10^{-7}$ W/m² K (Fig. 11(a)). If no TBR is considered for the same $(dn/dT)_{GaNonSiC} = 5.2 \times 10^{-5}$ K^{-1}, the calculated and measured data differ by ~30%; see Fig. 11(b). The contributions of phase shift coming from GaN and SiC are also given in the graphs. If TBR is included (Fig. 11(a)) the phase shift arises mostly from GaN where the heat is confined, and this is in contrast to the case of TBR = 0 (Fig. 11(b)).

In Fig. 12 we demonstrate the role of TBR values for different substrates by calculating the steady-state temperature profiles in the cross-sections of TLM devices at $P_{2D} =$

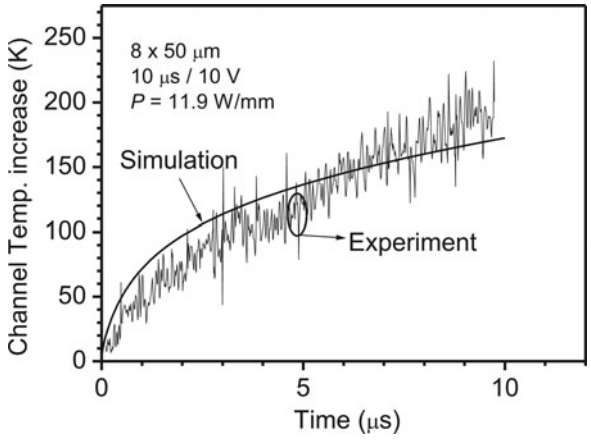

Fig. 9. Calculated and experimental time evolution of the temperature increase in the channel of HEMT during the 10 V pulse. After [22].

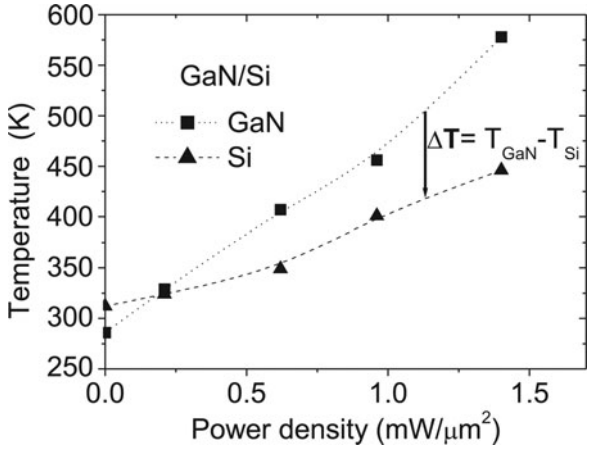

Fig. 10. Micro-Raman measurements of the temperature discontinuity at the GaN/Si interface in the steady-state in AlGaN/GaN/Si TLM structure. After [23].

https://doi.org/10.1017/S1759078709990444 Published online by Cambridge University Press

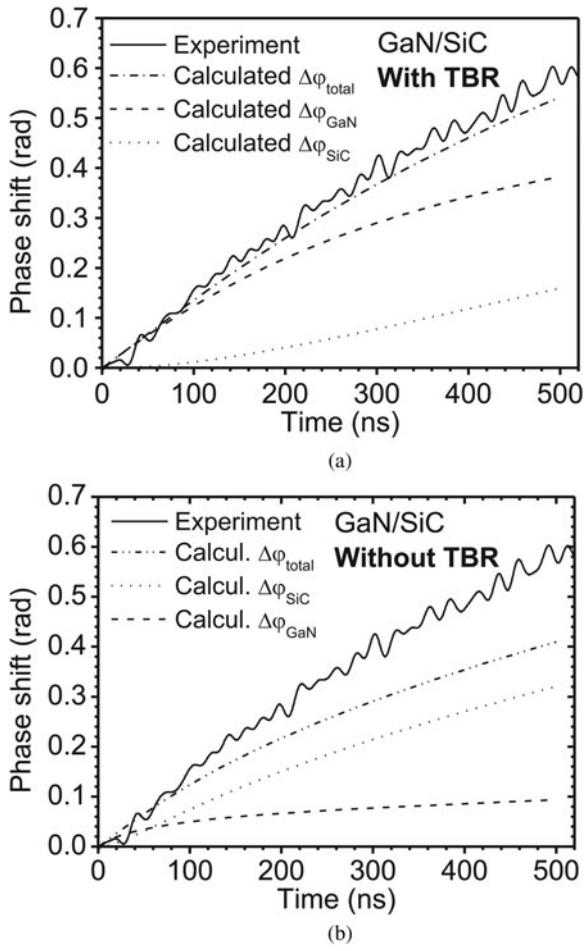

Fig. 11. Comparison of calculated $\Delta\varphi_{total}(t)$ with experimental TIM $\Delta\varphi(t)$ for $P_{2D} \sim 8.25$ mW/μm² in AlGaN/GaN/SiC TLM structure for (a) $(TBR)_{GaN/SiC} = 1.2 \times 10^{-7}$ W/m²K, $(dn/dT)_{GaNonSiC} = 5.2 \times 10^{-5}$ K^{-1} and (b) $(TBR)_{GaN/SiC} = 0$, $(dn/dT)_{GaNonSiC} = 5.2 \times 10^{-5}$ K^{-1}. After [23].

1 mW/μm². The III-nitride/substrate interface is located 1.2 μm from the surface for all structure types. For clarity the temperature profiles are shown only down to 5 μm from the surface. We assume $k_{Si} = 150$ W/mK [26]. For the GaN/SiC interface we used the above-obtained TBR = 1.2×10^{-7} m²K/W; similarly, for GaN/Si we used the previously determined value of 7×10^{-8} m²K/W, and for GaN/sapphire we tested TBR = 1.2×10^{-7} m²K/W. As expected, the highest surface temperature T_{surf} was obtained for GaN grown on sapphire (~810 K), while the smallest value was obtained for SiC substrate (~420 K). However, the influence of TBR on device thermal performance, well represented by ratio $\Delta T/T_{surf}$, is the highest for SiC (~65%) and the lowest for sapphire (~10%).

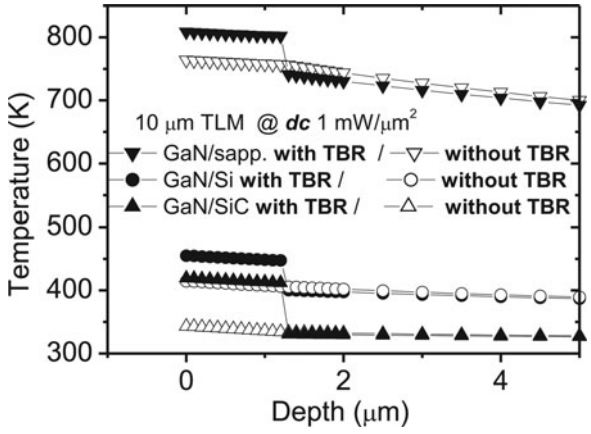

Fig. 12. Calculated steady-state temperature cross-section profiles in TLM structures on different substrates. Profiles are calculated for $P_{2D} = 1$ mW/μm² with $(TBR)_{GaN/SiC} = (TBR)_{GaN/sapphire} = 1.2 \times 10^{-7}$ W/m²K, $(TBR)_{GaN/Si} = 7 \times 10^{-8}$ W/m²K and without considering TBR. After [23].

IV. CONCLUSIONS

We have developed a transient electrical characterization method for the determination of HEMT channel temperature. Experimentally obtained channel temperature values were correlated with the results of the 2D thermal model, implying the presence of a TBR of about 7×10^{-8} m²K/W at the GaN/silicon junction.

We studied transient self-heating effects in the multifinger AlGaN/GaN/sapphire HEMT with the airbridge structure connecting sources. We showed that the airbridge structure absorbs the heat and the HEMT thermal design may be optimized for a given pulsed regime. The cooling efficiency of the airbridge structure increases with the time and saturates at ~6 μs, taking away ~10% of the heat.

We experimentally investigated TBR between GaN and Si, SiC, and sapphire. We found TBR to be $\sim 7 \times 10^{-8} \pm 20\%$ m²K/W at the GaN/Si interface and $\sim 1.2 \times 10^{-7} \pm 50\%$ m²K/W at the GaN/SiC interface. It is difficult to estimate TBR at the GaN/sapphire interface; however, in this case the role of TBR was shown to be less important.

ACKNOWLEDGEMENT

This work was supported by the TARGET-"Top Amplifier Research Groups in a European Team" project of the Information Society Technologies Program of the EU under contract IST-1-507893-NOE.

REFERENCES

[1] Shin, M.W.; Trew, R.J.: GaN MESFETs for high-frequency and high-temperature microwave applications. Electronics Letters., **31** (1995), 498–500.

[2] Daumiller, I.; Kirchner, C.; Kamp, M.; Ebeling, K.J.; Kohn, E.: Evaluation of the temperature stability of AlGaN/GaN heterostructure FET's. IEEE Electron Device Lett., **20** (1999), 448–450.

[3] Kohn, E.; Daumiller, I.; Kunze, M.; Nostrand, J.; Van Sewell, J.; Jenkins, T.: Switching behaviour of GaN-based HFETs: thermal and electronics transients. Electron. Lett., **38** (2002), 603–605.

[4] Kohn, E. *et al.*: Transient characteristics of GaN-based heterostructure field-effect transistors. IEEE Trans. Microwave Theory Tech., **51** (2003), 634–641.

[5] Gaska, R.; Osinsky, A.; Yang, J.W.; Shur, M.S.: Self-heating in high-power AlGaN-GaN HFET's. IEEE Electron Device Lett., **19** (1998), 89–91.

[6] Zhao, Y. *et al.*: Pulsed photothermal reflectance measurement of the thermal conductivity of sputtered aluminium nitride thin films. J. Appl. Phys., **96** (2004), 4563–4568.

https://doi.org/10.1017/S1759078709990444 Published online by Cambridge University Press

[7] Filippov, K.A.; Balandin, A.A.: The effect of the thermal boundary resistance on self-heating of AlGaN/GaN HFETs. MRS Internet J. Nitride Semiconductor Res. [Online]. 8, article 4. Avaliable at: http://nsr.mij.mrs.org/8/4/, (2003).

[8] Turin, V.O.; Balandin, A.A.: Performance degradation of GaN field-effect transistors due to thermal boundary resistance at GaN/substrate interface. Electron. Lett., **40** (2004), 81–83.

[9] Eckhause, T.A.; Süzer, Ö.; Kurdak, C.; Yun, F.; Morkoc, H.: Electric-field-induced heating and energy relaxation in GaN. Appl. Phys. Lett., **82** (2003), 3035–3037.

[10] Liu, R.; Ponce, F.A.; Dadgar, A.; Krost, A.: Atomic arrangement at the AlN/Si (111) interface. Appl. Phys. Lett., **83** (2003), 860–862.

[11] Sun, J. *et al.*: Thermal Management of AlGaN-GaN HFETs on sapphire using flip-chip bonding with epoxy underfill. IEEE Electron Dev. Lett., **24** (2003), 375–377.

[12] Das, J. *et al.*: Improved thermal performance of AlGaN/GaN HEMTs by an optimized flip-chip design. IEEE Trans. Electron Devices, **53** (2006), 2696–2702.

[13] Kuball, M. *et al.*: Measurement of temperature distribution in multi-finger AlGaN/GaN heterostructure field-effect transistors using micro-Raman spectroscopy. Appl. Phys. Lett., **82** (2003), 124–126.

[14] Shigekawa, N.; Onodera, K.; Shiojima, K.: Device Temperature measurement of highly biased AlGaN/GaN high-electron-mobility transistors. Jpn. J. Appl. Phys., **42** (2003), 2245–2249.

[15] Kuzmík, J.; Pogany, D.; Gornik, E.; Javorka, P.; Kordoš, P.: Electrostatic discharge effects in AlGaN/GaN high-electron-mobility transistors. Appl. Phys. Lett., **83** (2003), 4655–4657.

[16] Park, J.; Shin, M.W.; Lee, Ch.C.: Thermal modeling and measurement of AlGaN-GaN HFETs built on sapphire and SiC substrates. IEEE Trans. Electron Devices, **51** (2004), 1753–1759.

[17] Kuzmík, J.; Javorka, P.; Alam, A.; Marso, M.; Heuken, M.; Kordoš, P.: Determination of channel temperature in AlGaN/GaN HEMTs grown on sapphire and silicon substrates using DC characterization method. IEEE Trans. Electron Devices, **49** (2002), 1496–1498.

[18] Brown, J.D.; Borges, R.; Piner, E.; Vescan, A.; Singhal, S.; Therrien, R.: AlGaN/GaN HFETs fabricated on 100-mm GaN on silicon (111) substrates. Solid-State Electronics., **46** (2002), 1535–1539.

[19] Pogany, D. *et al.*: Quantitative internal thermal energy mapping of semiconductor devices under short current stress using backside laser interferometry. IEEE Trans. Electron Devices, **49** (2002), 2070–2078.

[20] Pogany, D.; Bychikhin, S.; Litzenberger, M.; Groos, G.; Stecher, M.: Extraction of spatio-temporal distribution of power dissipation in semiconductor devices using nanosecond interferometric mapping technique. Appl. Phys. Lett., **81** (2002), 2881–2883.

[21] Kuzmik, J. *et al.*: Transient thermal characterization of AlGaN/GaN HEMTs Grown on silicon. IEEE Trans. Electron Devices, **52** (2005), 1698–1705.

[22] Kuzmik, J. *et al.*: Transient self-heating efects in multifinger AlGaN/GaN HEMTs with metal airbridges. Solid-State Electronics, **51** (2007), 969–974.

[23] Kuzmik, J.; Bychikhin, S.; Pogany, D.; Gaquière, C.; Pichonat, E.; Morvan, E.: Investigation of the thermal boundary resistance at the III-nitride/substrate interface using optical methods. J. Appl. Phys., **101** (2007), 054508.

[24] Pichonat, E. *et al.*: Temperature analysis of AlGaN/GaN high-electron-mobility transistors using micro-Raman scattering spectroscopy and transient interferometric mapping. European Microwave Week, Manchester, 10–15 September (2006).

[25] Balkanski, M.; Wallis, R.F.; Haro, E.: Anharmonic effects in light scattering due to optical phonons in silicon. Phys. Rev. B, **28** (1983), 1928–1934.

[26] Hull, R, editor, Properties of Crystalline Silicon. EMIS Datareviews Series No. 20, INSPEC, 1999.

Jan Kuzmik received Ph.D. from the Slovak Academy of Sciences in 1991. From 1991 till 1994 he was a research fellow at the Institute of Electronic Structure and Laser, Heraklion, Greece. From 1994 he is with the Slovak Academy of Science, from 1996 till 1998 he had been awarded a JSPS Fellowship at the Kyoto Institute of Technology, Japan. Since 2002 he works also at the Institute for Solid State Electronics, TU Wien. His interest includes technology of III–V devices, SiC, GaN HEMTs, and characterization of high-power devices. He is author or co-author of more than 80 scientific papers. He is author of the European project ULTRAGAN on InAlN/GaN power electronics. He chaired EuroConference ASDAM 2000, reviews *Journal of Applied Physics*, *IEEE Electron Dev. Lett.* as well as *Trans. on Electron Dev.*

Sergey Bychikhin received his M.Sc. (1995) and Ph.D. (2000) degrees from Physics Department of the M.V. Lomonosov Moscow State University, Russia. Since 2000 he joined the group for semiconductor device characterization in the Institute for Solid State Electronics in the Vienna. He is engaged in the field of the thermal and free carrier analysis of the ESD protection structures by backside laser interferometry. His current research interests are in the device characterization and simulation during the HBM and CDM stress.

Dionyz Pogany received his Dipl. - Ing. degree in Solid State Engineering from the Slovak Technical University in Bratislava in 1987. In 1994 he received a Ph.D. degree at INSA de Lyon, France. In 1994–1995 he was a postdoc at France Telecom, CNET-Grenoble. Since 1995 he is with the Institute of Solid State Electronics, TU Vienna, Austria, where he leads a research team. Since 2003 he is Associate Professor at TU Vienna. He has published on defect states in semiconductors, low-frequency noise, device physics and reliability physics. His current research interest is in electrostatic discharge (ESD) phenomena, current filamentation, self-heating effects and device reliability physics of Si power electronics, ESD protection devices, GaN-based HEMTs and LEDs, and development of new optical methods for device characterization and failure analysis. He is author or co-author of more than 220 scientific papers. He has been managing several R&D projects.

https://doi.org/10.1017/S1759078709990444 Published online by Cambridge University Press

Dr. Kohn earned his Ph.D. at the Technical University of Aachen (Germany) in 1975. After postdoc studies at the University of Newcastle upon Tyne in the UK and many years in industry in Germany (at AEG Telefunken), France (Thomson CSF), and the US (Siemens) he joined the University of Ulm as professor and Director of the Institute of Electron Devices and Circuits in 1989, also serving as director of the Microelectronics Technology Centre. His research activities include design and technology of advanced electronic device structures in a number of semiconductors, like recently III-nitride heterostructures and diamond for high-temperature, high-power, and high-speed applications. This is accompanied by work on advanced packaging technologies and MEMS sensor and actuator devices, mainly based on CVD diamond for RF applications and applications in electrochemistry and life science. He is a member of the IEEE and Electrochemical Society and has served as IEEE distinguished lecturer. He has been a visiting fellow to the University of Wales (GB), the Norwegian Institute of Technology (Trondheim, Norway), Cornell University (NY), the National Cheng Kung University in Tainan (Taiwan), and the Air Force Research Laboratories in Dayton (OH), and has been an Adjunct Professor of Physics at the New Jersey Institute of Technology, Newark (NJ). He is the Director of the Steinbeis Technology Transfer Centre "Semiconductor Devices"; and his activities have led to two spin-off companies, GFD (Gesellschaft für Diamantprodukte) and MicroGaN.

Emmanuelle Pichonat received her Engineer Diploma in 1998 from the ESIREM School, Dijon, France. She received the Ph.D. degree from the University of Sciences and Technologies of Franche-Comté, Besançon, France in 2002. From 2003 to 2004, she was a post-doctoral fellow at IEMN, Lille, France. Since 2004, she has been an assistant professor at the LASIR in Lille. Her current research interest is the characterization of III–V devices, HEMTs, and high-power devices by micro-Raman scattering spectroscopy.

Christophe Gaquière, professor at the University of Lille, carries out his research activity at the Institut d'Electronique de Microélectronique et de Nanotechnology (IEMN). The topics concern design, fabrication, and characterization of HEMT and HBT devices. He works on GaAs, InP, metamorphic, and GaN HEMTs. His main activities are microwave characterizations (small and large signal between 1 and 325 GHz) in order to correlate the microwave performances with the technological and topology parameters. Today, his activities concern the investigation of two-dimensional electronic plasmons for THz solid state GaN-based detectors and emitters and AlGaN/GaN nanowires for microwave applications. He was responsible for the microwave characterization part of the common laboratory between Thales TRT and IEMN focus on wide band gap semiconductor (GaN, SiC, and Diamond) up to 2007. At the present time he has in charge the Silicon millimeter wave advanced technologies part of the common lab between ST microelectronics and IEMN. Christophe Gaquière is author or co-author of more than 70 publications and 150 publications.

Erwan Morvan was born in Garmisch in 1971. He first graduated in material physics and semiconductor devices at National Institue for Applied Science (INSA) in Lyon (France). From 1995 to 1999 he was a Ph.D. student at National Center for Microelectronics in Barcelona (CNM). He was active in the field of device and technology simulation and he developed an ion implantation simulator for silicon carbide (SiC) crystal. He got Ph.D. in Electronics from INSA Lyon in 1999. In 2000, he joined the Corporate Laboratory of Thomson CSF (LCR), now called Thales Research and Technology (TRT). From 2000 to 2003, he was involved in SiC MESFET design, technology, and characterization as a research engineer. Since 2003 he has been working on GaN-based high-power/high-frequency devices. He is head of the GaN devices processing team at Alcatel-THALES III-Vlab since 2008.

Jean-Pierre Teyssier was born in 1963 in Brive, France. Since 1990, he works at the IRCOM/XLIM lab of the University of Limoges, France, in the group of Pr Raymond Quéré. He has presented his Ph.D. thesis in 1994, the subject was about pulsed *I(V)* and pulsed S-Parameters for nonlinear characterization of microwave active devices. Up to now, he is involved in the design of measurement systems and instrumentation for microwave nonlinear investigations, with an emphasis on time domain pulsed large signal characterization of transistors. Since many years, Jean-Pierre Teyssier and his students are frequent contributors of ARFTG papers, and he has been in fall 2006 the organizer of the ARFTG workshop about RF samplers. He has defended in 2007 his habilitation thesis in order to become a full university professor. He is now a member of ARFTG ExCom, responsible for workshop organization.

https://doi.org/10.1017/S1759078709990444 Published online by Cambridge University Press